AD NUMBER

ADB270749

NEW LIMITATION CHANGE

TO

Approved for public release, distribution unlimited

FROM

Distribution authorized to U.S. Gov't. agencies only; Proprietary Info.; Apr 2001. Other requests shall be referred to U.S. Army Medical Research and Materiel Command, 504 Scott St., Fort Detrick, MD 21702-5012.

AUTHORITY

USAMRMC ltr, dtd 15 May 2003

AD_____

Award Number: DAMD17-98-1-8551

TITLE: Structure and Interactions of a Protein Linked to Apoptosis as Response in Prostate Tumors

PRINCIPAL INVESTIGATOR: Steven M. Pascal, Ph.D.

CONTRACTING ORGANIZATION: University of Rochester
Rochester, New York 14627

REPORT DATE: April 2001

TYPE OF REPORT: Final

PREPARED FOR: U.S. Army Medical Research and Materiel Command
Fort Detrick, Maryland 21702-5012

NOTICE

USING GOVERNMENT DRAWINGS, SPECIFICATIONS, OR OTHER DATA INCLUDED IN THIS DOCUMENT FOR ANY PURPOSE OTHER THAN GOVERNMENT PROCUREMENT DOES NOT IN ANY WAY OBLIGATE THE U.S. GOVERNMENT. THE FACT THAT THE GOVERNMENT FORMULATED OR SUPPLIED THE DRAWINGS, SPECIFICATIONS, OR OTHER DATA DOES NOT LICENSE THE HOLDER OR ANY OTHER PERSON OR CORPORATION; OR CONVEY ANY RIGHTS OR PERMISSION TO MANUFACTURE, USE, OR SELL ANY PATENTED INVENTION THAT MAY RELATE TO THEM.

LIMITED RIGHTS LEGEND

Award Number: DAMD17-98-1-8551
Organization: University of Rochester

Those portions of the technical data contained in this report marked as limited rights data shall not, without the written permission of the above contractor, be (a) released or disclosed outside the government, (b) used by the Government for manufacture or, in the case of computer software documentation, for preparing the same or similar computer software, or (c) used by a party other than the Government, except that the Government may release or disclose technical data to persons outside the Government, or permit the use of technical data by such persons, if (i) such release, disclosure, or use is necessary for emergency repair or overhaul or (ii) is a release or disclosure of technical data (other than detailed manufacturing or process data) to, or use of such data by, a foreign government that is in the interest of the Government and is required for evaluational or informational purposes, provided in either case that such release, disclosure or use is made subject to a prohibition that the person to whom the data is released or disclosed may not further use, release or disclose such data, and the contractor or subcontractor or subcontractor asserting the restriction is notified of such release, disclosure or use. This legend, together with the indications of the portions of this data which are subject to such limitations, shall be included on any reproduction hereof which includes any part of the portions subject to such limitations.

THIS TECHNICAL REPORT HAS BEEN REVIEWED AND IS APPROVED FOR PUBLICATION.

Nmishacha Mann
08/18/01

REPORT DOCUMENTATION PAGE

Form Approved
OMB No. 074-0188

1. AGENCY USE ONLY (Leave blank)	2. REPORT DATE	3. REPORT TYPE AND DATES COVERED
	April 2001	Final (1 Oct 98 - 31 Mar 01)

4. TITLE AND SUBTITLE
Structure and Interactions of a Protein Linked to Apoptosis as Response in Prostate Tumors

5. FUNDING NUMBERS
DAMD17-98-1-8551

6. AUTHOR(S)
Steven M. Pascal, Ph.D.

7. PERFORMING ORGANIZATION NAME(S) AND ADDRESS(ES)
University of Rochester
Rochester, New York 14627

E-Mail: pascal@oxbow.biophysics.rochester.edu

8. PERFORMING ORGANIZATION REPORT NUMBER

9. SPONSORING / MONITORING AGENCY NAME(S) AND ADDRESS(ES)
U.S. Army Medical Research and Materiel Command
Fort Detrick, Maryland 21702-5012

10. SPONSORING / MONITORING AGENCY REPORT NUMBER

11. SUPPLEMENTARY NOTES

12a. DISTRIBUTION / AVAILABILITY STATEMENT
Distribution authorized to U.S. Government agencies only (proprietary information, Apr 01). Other requests for this document shall be referred to U.S. Army Medical Research and Materiel Command, 504 Scott Street, Fort Detrick, Maryland 21702-5012.

12b. DISTRIBUTION CODE

13. ABSTRACT *(Maximum 200 Words)*

Androgen ablation can be used to induce apoptosis of certain cancerous prostate cells. Unfortunately, a fraction of prostate cells are androgen-indepependent and thus resist treatment, leading to a relapse of disease. Par-4 is a protein found to be upregulated in mammalian prostate cancer cells induced to undergo apoptosis, and its presence in both androgen-dependent and androgen-independent prostate cells could be an avenue for inducing apoptosis of the resistant cells. In order to investigate the structure/function relationship of Par-4, we have performed CD and NMR studies of the C-terminus of this molecule, a region which is responsible for self-association and association of Par-4 with effector molecules. We have shown that the C-terminus exists in equilibrium between an unstructured monomer and a coiled coil structure, and that reduction in pH and temperature can dramatically shift this equilibrium to favor the coiled coil. The pH requirements for coiled coil formation may be related to the fact that Par-4 has been found to interact with endosome-associated proteins.

14. SUBJECT TERMS

15. NUMBER OF PAGES
28

16. PRICE CODE

17. SECURITY CLASSIFICATION OF REPORT	18. SECURITY CLASSIFICATION OF THIS PAGE	19. SECURITY CLASSIFICATION OF ABSTRACT	20. LIMITATION OF ABSTRACT
Unclassified	Unclassified	Unclassified	Unlimited

Table of Contents

INTRODUCTION

The prostate apoptosis response – 4 (Par-4) protein was first identified by differential screening for upregulated genes in prostate cancer cells undergoing apoptosis (*1*). Par-4 expression has since been detected in diverse tissue types (*2*), and its upregulation in neurons has been linked to a variety of neurodegenerative disorders, including Alzheimer's (*3*), Huntington's (*4*) and Parkinson's (*5*) diseases, HIV encephalitis (*6*) and amylotrophic lateral sclerosis (*7*). Downregulation of Par-4 has been linked to several cancers, including those of the prostate (*1, 8*), colon (*9*) and kidney (*10*). The primary sequence of the Par-4 protein contains a heptad repeat at the C-terminus (Figure 1) which strongly suggests the presence of a leucine zipper (LZ), and is essential for the ability of Par-4 to lower the apoptotic threshold of cells (*8*), as well as for the ability of Par-4 to self associate and interact with various proposed effector molecules (*11-13*). For instance, the LZ domain has been shown to bind to the zinc-coordinating regulatory domain of two atypical isoforms of protein kinase C (*11*). The resulting downregulation of aPKC activity has been proposed as the pathway through which Par-4 induces increased sensitivity to apoptotic stimuli (*11*). Various other interactions have been investigated in order to further elucidate the role of Par-4 in apoptosis and cancer, resulting in linkage of Par-4 to Bcl-2, NF-κB/IF-κB (*14-16*), and the Ras oncogene pathway (*17-19*). The original goal of this proposal was to determine the oligomerization state and three-dimensional structure of the Par-4 C-terminus, and to and begin to characterize the interaction between this region of Par-4 and various effector molecules, including the aPKCs. We have succeeded in showing that the Par-4 C-terminus is natively unfolded at physiological pH and temperature, but can be induced to form a coiled coil at low pH and low temperature. Furthermore, salt helps to stabilize the coiled coil at high pH, but is destabilizing at low pH, and the two state conformational equilibrium is affected by peptide concentration. We will discuss these observations in terms of the primary sequence of the Par-4 LZ domain, and suggest how the pH-dependent behavior of Par-4 correlates with its proposed physiological role in induction of apoptosis.

BODY

Methods

Expression and purification of the Par-4 C-terminal peptide

The Par-4 LZ, comprising residues 286-332 of racine Par-4, was subcloned into the H-MBP-3C vector (*20*). Following previously described expression and purification of the resulting MBP-fusion protein and fusion cleavage with recombinant protease (*20*), the eluted Par-4 protein was dialyzed against an aqueous buffer containing 12mM NaP_i at pH 7.5. An additional ion exchange purification step was performed with a Hi-Trap Q Sepharose column (Amersham-Pharmacia). The protein was eluted with an increasing NaCl gradient, and exchanged into aqueous buffer containing 20mM NaCl, 12mM NaP_i, pH 6.5. SDS-PAGE and MALDI mass spectroscopy showed the protein to be >99% pure. The amino acid composition was confirmed and the concentration was determined by amino acid analysis.

Circular dichroism (CD) spectroscopy

CD spectra were recorded on an AVIV model 202 CD spectrometer equipped with a thermoelectric sample temperature controller and a 0.1 cm pathlength cuvette. Spectra were recorded in 0.5 nm steps from 260 to 190 nm with an integration time of 2 seconds at each wavelength, and baseline corrected against a cuvette containing buffer alone. Estimates of the fractional helicity were made using either $[\Theta_{222}]$/-35,000 (*21*) or the SELCON program (*22*), which analyzes CD spectra for α-helical, β-sheet and other content (includes random coil and turn conformations), using a database of spectra from 48 proteins of known secondary structure. These two methods agree to within 5% for all studies reported here, and so will not be distinguished in the discussions below. Thermal stability was determined by monitoring the molar ellipticity at 222 nm as a function of temperature at 5°C intervals with 5 minutes equilibration and a collection time of 30 sec at each temperature. No significant irreversibility of CD spectra was detected when temperature, pH, salt concentration or peptide concentration was cycled, provided that peptide precipitation at low pH was avoided.

Extraction of thermodynamic parameters via non-linear least square best fitting of a two state model (2 unfolded monomers folded dimer) closely followed the work of Bosshard and colleagues (*23-25*). Variation of molar ellipticity and fractional helicity with pH was used to extract values of the conformational pKa and the Hill coefficient (n), at various temperatures and salt concentrations, via a modified form of the Henderson-Hasselbalch equation:

$$[\Theta]_{obs} = \frac{[\Theta_D] + [\Theta_M]10^{n(pH-pKa)}}{1 + 10^{n(pH-pKa)}} \qquad (1)$$

where the known variables are the observed molar ellipticity at 222 nm ($[\Theta]_{obs}$) and the pH. Fitting also yielded the values of $[\Theta_D]$ and $[\Theta_M]$, the extrapolated plateau values of molar ellipticity at 222 nm at the acidic and basic pH limits (where the subscript denotes dimer or monomer).

Variation of molar ellipticity with temperature was used to extract values of T_m, the characteristic melting temperature, and ΔH_m, the enthalpy of melting, at 5 different pH values, three different salt concentrations and various peptide concentrations via the following procedure:

The observed molar ellipticity can be related to the plateau values by:

$$[\Theta]_{obs} = f_M[\Theta_M] + (1-f_M)[\Theta_D] \quad (2)$$

where f_M is the fractional population of the monomer state. Equation 2 can be rearranged to:

$$f_M = \frac{[\Theta]_{obs} - [\Theta_D]}{[\Theta_M] - [\Theta_D]} \quad (3)$$

By definition, $K_d = [M]^2/[D]$, $[M] = f_M C_{tot}$ and $[D] = C_{tot}(1-f_M)/2$, and thus:

$$K_d = \frac{2f_M^2 C_{tot}}{1-f_M} \quad (4)$$

where K_d is the dissociation constant, and C_{tot} is the total peptide concentration. Equation 4 can be solved for f_M via the quadratic equation:

$$f_M = \frac{-K_d + \mathrm{sqrt}(K_d^2 + 8C_{tot}K_d)}{4C_{tot}} \quad (5)$$

Equation 5 can be rendered into a useful form by substituting the expression for f_M from equation 3, and also substituting the following expression for K_d, which assumes that ΔC_p, the change in heat capacity, is much less than ΔH_m (*23-25*):

$$K_d = C_{tot} \exp\left[\frac{\Delta H_m}{R}\left(\frac{1}{T_m} - \frac{1}{T}\right)\right] \quad (6)$$

After the temperature dependence of $[\Theta_D]$ is introduced by substituting $[\Theta_D] = [\Theta_{D0}] + \gamma T$, the modified equation 5 can be solved for $[\Theta]_{obs}$ and then used to fit experimental melting curves such as those shown in Figure 6. Extracted parameters include T_m, ΔH_m, $[\Theta_{D0}]$, $[\Theta_M]$ and the constant γ.

NMR Spectroscopy

NMR spectroscopy was performed on a Varian INOVA 600 MHz spectrometer equipped with a triple resonance gradient probe. All data were processed with nmrPipe (*26*) and visualized and analyzed with NMRDraw (*26*) and NMRView (*27*). The final NMR sample was prepared by concentrating the purified Par-4 protein to 0.8 mM in 20mM NaCl, 12mM NaP, 5% (v/v) D_2O, 50μM NaN_3 and pH 6.5. All experiments were performed at 5°C with the proton carrier centered on the H_2O frequency (4.96 ppm) unless otherwise noted.

Two dimensional ^{1}H-^{15}N HSQC spectra were recorded as 2048 x 256 complex points with 8 scans per fid and recycle time of 1.2 sec. Sequence-specific assignments for Par-4 were done using HNCO (2048 x 64 x 20), CBCA(CO)NH, and HNCACB (2048 x 40 x 22) experiments. The side chain carbon and proton assignments were done using CCCONH (2048 x 60 x 32), HCCCONH (2048 x 64 x 16) and HCCH-TOCSY (2048 x 128 x 32). The proton sweep width was 6000 Hz. The carbon sweep width for HNCO experiments was 1250 Hz, and for CBCA(CO)NH, HNCACB, and CCCONH experiments were, 9000 Hz. The nitrogen sweep width was 1320 Hz in all the experiments except HNCO (900 Hz). The data were subsequently linear predicted in ^{15}N and ^{13}C dimension, zero filled and Fourier transformed to obtain 1024 x 256 x 128 complex points. All two and three dimensional data sets were apodized a with 30° shifted sine bell squared function in all dimensions.

Results

CD Spectroscopy

The thick trace in Figure 2 shows the CD spectrum of the PAR-4 LZ in 12mM NaP_i, 20 mM NaCl, pH 6.5 at 25°C. This spectrum represents an approximately 85% random coil structure (~15% helical). On lowering the temperature to -5°C (Figure 2, bottom trace), the helical content is increased to 37%, with the appearance of minima near 222 nm and 208 nm. The isodichroic point near 203 nm, which has been seen in the study of other leucine zippers, is commonly taken as evidence of a two state transition (*28-30*). Taken together, the data of Figure 2 suggest an equilibrium between a non-folded state and a marginally more stable helical state, which becomes somewhat increasingly favored at lower temperature.

In order to investigate the conformational variability further, CD spectra were taken over a range of pH values, with the temperature fixed at 5°C (Figure 3). The data indicate that acidic pH stabilizes helix formation. Fractional helicity increases from approximately 20% to 70% between pH 8.5 and pH 5.5. Next, the temperature was once again varied, but this time with the pH fixed at 5.75 (Figure 4). Lower temperature favors helix formation more markedly at this pH (compare Figure 2), with fractional helicity increasing from approximately 15% to 75% as the temperature decreases from 45 °C to 0 °C. Again, isodichroic points near 203 nm in Figure 3 and Figure 4 suggest a two state transition.

Plots of $[\Theta_{222}]$ vs. pH at 11 different temperatures are shown in Figure 5. Note that data was not acquired below pH 5.5 due to reduced peptide solubility. The data at each temperature was fit to equation 1 (see Materials and Methods) to yield values of the conformational pKa, which is the characteristic pH at the transition midpoint, and the Hill coefficient, indicating the degree of cooperativity. Results are tabulated in Table 1, and pKa values are depicted graphically in the Figure 5 inset. Fitting at higher temperatures requires considerable extrapolation, and results in large uncertainties. Therefore, these values are not plotted in the inset. However, it is clear that at least at low temperature, the apparent pKa decreases in a regular fashion as temperature increases, and the Hill coefficients of approximately 2 imply cooperative folding as a function of pH.

Plots of $[\Theta_{222}]$ vs. temperature in 20 mM NaCl at 5 different pH values are shown in Figure 6. The values of T_m and ΔH_m, the characteristic melting temperature and the enthalpy of melting, were extracted as described in Materials and Methods. The results are shown in Table 2, along with similar results for two other salt concentrations. T_m decreases from approximately 35 °C to –1 °C as the pH increases from 5.5 to 8.0 (Figure 6, inset). The decrease of T_m with pH is very steep at pH 6 and below, and flattens out somewhat at high pH, where titration of acidic groups should be complete. Note though that fitting is less reliable at high pH.

The conformation is also sensitive to salt concentration. Figure 7 shows the variation in fractional helicity as a function of pH, at 3 different NaCl concentrations at 5 °C. At pH 8.5, 20 mM NaCl results in only 13% helical content, while increasing NaCl concentration to 80 or 140 mM increases the helical content to 22%. The situation is reversed at pH 5.5, where 20 and 80 mM salt induces approximately 80% helix, while increasing the salt concentration to 140 mM decreases the helical content to 70%. The data was fit to equation 1 in a similar manner as the curves from Figure 5, with fractional helicity replacing molar ellipticity. The resulting pKa values are in the range of 6.14 ± 0.05 for each salt concentration, which is consistent with the values extracted for the 5 °C curve of Figure 5 (Table 1). The Hill coefficients are again near 2, although the value for the 20 mM NaCl curve is 2.86 ± 0.35, while the Hill coefficients for the 80 mM and 140 mM NaCl curves fall just below 2. Thus it appears that low salt marginally increases the cooperativity of the transition. It should be noted that the increase in the calculated cooperativity is correlated with the wider disparity between the plateau values of fractional helicity at 20 mM NaCl. Thermal stability, as measured by T_m, appears to follow a similar trend (Table 2), with high salt somewhat favoring helix formation at high pH, while low salt is marginally stabilizing at low pH.

The concentration dependence of the Par-4 peptide conformation was investigated. At each of the three pH values represented in the Figure 8, increasing peptide concentration resulted in increased thermal stability (increased T_m). T_m values for pH 6.5 were extracted from higher concentration samples, since extraction of T_m values at low concentration and high pH is inaccurate (see Figure 6, top 2 curves). Note that $1/T_m$ as a function of $\ln(C_{tot})$ is approximately linear (Figure 8 inset), consistent with a two-state transition at each pH value (*23, 31*).

NMR Spectroscopy

Chemical shift assignments of the PAR-4 peptide are listed in Table 3, and backbone HN and 15N assignments are indicated also in Figure 10. The procedure of assigning the backbone is briefly documented in Figure 11. The Par-4 LZ peptide is highly soluble at pH 6.5, in the presence of minimal salt. NMR spectra (see Figure 9) display little chemical shift dispersion. Dispersion is expected to be minimal in either a random coil or a purely alpha helical peptide, particularly in the absence of aromatic residues. To assign the backbone resonances of the peptide, standard triple resonance techniques were used. Analysis of HNCO, CBCA(CO)NH and HNCACB experiments (Figure 3) allowed assignment of nearly all HN,N,C',Ca,Cb resonances (supplemental materials). A CCC-TOCSY-NH experiment was used to confirm and clarify the assignments. Chemical shift indexing (*32, 33*) suggests that little stable structure exists under these sample conditions. The value of most $^{3}J_{HNHa}$ coupling constants is between 6 and 7 Hz, again indicating little if any stable secondary structure, consistent with CD spectra at high pH. But assignments at this pH will serve as a starting point for assignment at lower pH, as the sample will be titrated, and migration of peaks as pH changes will be followed.

Discussion

Coiled coils are amphipathic helical oligomerization motifs found in many types of proteins (*34-36*). In naturally occurring dimeric forms, two α-helices coil around each other with a slight left handed superhelical twist. The amino acid sequence can be organized into a seven residue repetitive heptad pattern, designated $(abcdefg)_n$, in which *a* and *d* positions are generally hydrophobic and are present at the center of the oligomeric interface. The most common hydrophobic residues at these positions are Leu, Val, and Ile. Coiled coils with predominantly Leu at position *d* are known as leucine zippers (LZ). Asn is also quite common at the *a* position, and its presence has been correlated with the occurrence of a parallel dimeric state (*37-43*). The solvent exposed *b*, *c* and *f* positions affect stability, solubility and the specificity of interactions with other molecules, but do not appear to affect the fold or interhelical orientation as strongly as the *a,d,e* and *g* residues (*44-46*).

Although hydrophobic interactions at the oligomeric interface are the principal driving force for folding and oligomerization of coiled coils, electrostatic interactions can also contribute significantly to stability and instability. For instance, charged side chains in the *e* and *g* positions can interact with the opposite strands (*g'* and *e'*). These interactions can be complimentary or non-complimentary depending on the type of residues present at the *e* and *g* positions. While questions remain regarding the contributions to stability from complimentary interactions, it is clear that charge clashes such as between two acidic side chains can have a profound affect upon both the stability and stoichiometry of coiled coils (*23, 24, 29, 30, 47-50*).

The present studies were conducted with a 51 residue peptide, representing the C-terminal 47 residues of Par-4 (residues 286-332) preceded by a four residue cloning artifact. For simplicity, these residues have been redesignated residues 1-51. Residues 11-51 are depicted in helical wheel format in Figure 1. Orienting the heptad repeat by placing the Leucine repeat at the

d position results in an additional hydrophobic repeat at the *a* position, with the exception of two Asn residues, which suggest the presence of a parallel coiled-coil dimer structure. The distribution of L predominantly at *d* and I at *a* also suggests a propensity to form a dimeric coiled-coil, whereas reversal of this pattern would be consistent with tetrameric coil formation (*39*). Our experimental results are consistent with these sequence-based predictions, although the oligomeric state and interhelical orientation have not been determined explicitly. The experimental evidence for environment-dependent coiled-coil formation is discussed below.

Helicity, two state cooperative transition, $[\Theta_{222}]/[\Theta_{208}]$: CD spectra indicate that the PAR-4 LZ peptide forms a predominantly alpha helical structure at low pH and low temperature (Figure 3 and 4, lower traces). While this alone is not sufficient to specify a coiled coil, conformationally stable isolated helices in aqueous solution are rare in the absence of helix favoring conditions such as less polar solvents (51, 52). It is well known that in coiled coils, helix formation and interhelical assembly are commonly tightly coupled, and the presence of isolated helices is rarely detected (28, 53-57). This folding pathway therefore represents an equilibrium between just two predominant states: the unfolded monomer and the coiled-coil dimer, with no detectable intermediate. Thus, evidence of a two state transition is further evidence of coiled-coil formation. As noted previously, the isodichroic points near 203 nm in Figures 2, 3 and 4 are characteristic of a two state transition, and further support is supplied by the ability to fit the curves of Figures 5, 6 and 7 with a two state model (see Materials and Methods). The Hill coefficients of these curves indicate that the transition is cooperative. Note also that $[\Theta_{222}]$ becomes more negative than $[\Theta_{208}]$ at maximal helicity (Figure 3 and 4, lower traces). The value of the $[\Theta_{222}]/[\Theta_{208}]$ ratio for non-coiled helices is typically near 0.83. For alpha helices which are part of a coiled coil structure, the parallel polarized amide $\pi-\pi^*$ transition becomes less dichroic, effectively reducing the negativity of $[\Theta_{208}]$. Since $[\Theta_{222}]$ is unaffected, the $[\Theta_{222}]/[\Theta_{208}]$ ratio increases to approximately 1.03. Hence the $[\Theta_{222}]/[\Theta_{208}]$ ratios of approximately 1.08 and 1.06 (bottom traces of Figure 3 and 4, respectively) are further confirmation of helical supercoiling (48, 58, 59).

Dependence on concentration, pH and salt: The concentration dependence of T_m shown in Figure 8 is a strong indication of intermolecular interactions, and is not consistent with the formation of non-interacting monomeric helices. The linearity seen in the inset graph is consistent with a two-state transition. The pH dependence is also consistent with coiled coil formation. In addition to a leucine repeat at position d, the sequence of the Par-4 LZ peptide has a strong acidic repeat at position g. In Figure 1, the two helical wheels have been aligned in a parallel symmetric fashion. Characteristically, parallel dimeric coiled coil side chains in the g position will make interhelical contact with e' side chains at the i+5 position (i.e. E17' with N22; also E17 with N22', where the prime indicates the second helical molecule). The role of polar interhelical contacts in coiled coil formation and stability has been much discussed (23, 24, 29, 30, 47-50). While the importance of complimentary (e.g. E31-K36') and neutral (e.g. E17'-N22 or E38'-L43) interactions appears to be case dependent, negative-negative interactions such as D24'-E29 have a considerable destabilizing affect upon helix formation. In the present case, it is likely that charge-charge repulsion between D24'and E29 (and the symmetric D24-E29' repulsion) is a major factor in disfavoring coiled-coil formation at high pH (Figure 3). However, it should also be noted that amino acids in the e position of coiled coils have been shown to interact intramolecularly with the b,c,d and f residues of the same heptad. Similarly, the g

position residues interact intramolecularly with the d and f positions of the same heptad, and the a and d residues of the next heptad (25). Thus, several intramolecular complimentary charge-charge interactions are expected to occur upon coil formation, including K15-E16, D24-R23 and K36-E33. Intramolecular negative-negative charge clashes include E17-E16, E31-D30, E29-D26 and E29-D30. The involvement of E29 in one interchain and two intrachain repulsions (actually six total repulsions in the symmetric dimer) suggest that this residue is a key to the pH-dependent folding of the Par-4 LZ, although each of the above listed contacts could contribute to helical instability at high pH.

Decrease in pH has been shown to increase the helicity of acidic coiled-coils, presumably due to at least partial protonation of one or more of the offending acidic side chain groups (*24, 28, 47, 48*). While the pKa of an acidic side chain normally falls in the 4.0-4.5 range, in a local environment containing other acidic groups, the pKa can be expected to increase, and pKa values of acidic side chains involved in *e-g* charge clashes in coiled coils have been shown to be elevated (*60-62*). This indicates a preference for protonation, which would abrogate the charge repulsion and allow the now neutral side chain to contribute to the stability of the hydrophobic core. These altered single group pKas can be reflected in the conformational pKa, although the exact nature of the correspondence has been difficult to establish. The conformational pKa values found here (Figure 5) are consistent with this explanation.

The salt dependence shown in Figure 7 further supports the importance of charge-charge interactions in folding of the Par-4 LZ. At high pH, the most important charge effects are the non-complimentary contacts: intermolecularly between D24' and E29 (also D24-E29'), and the intramolecular negative-negative clashes noted above. Increased salt concentration can help to screen the effects of these clashes, either by providing local counter-ions or by increasing the dielectric constant of the medium (*49, 63*). Accordingly, increasing salt concentration appears to increase helicity slightly. At low pH, one or more of the repulsive interactions has been reduced by at least partial protonation of one or more of the acidic groups. However, the "attractive" charge interactions, such as E31'-K36 may still be active, since acidic residues involved in stabilizing or marginally destabilizing interactions will have pKa values shifted to lower pH or to only slightly higher pH (*60-62*). Thus, at low pH, increasing salt can screen the remaining charge-charge interactions, which includes the attractive interactions and any remaining charge-charge repulsions which may remain,. This effect can also be described as an increase in desolvation penalty when the medium has a higher dielectric constant (*64*). It should be noted, however, that NaCl can have many and varied effects in solution, including salting out, which is widely recognized as a cause of protein and peptide aggregation and precipitation, but which can also simply encourage hydrophobic contacts to form at the dimer interface (*49, 65*). This dimeric salting out effect might tend to be more pronounced at low pH, since the dimer interface will be less charged. These and other effects must be carefully balanced in order to obtain a more complete picture of the effects of salt, pH, temperature, concentration and intrachain and interchain ionic effects upon coiled coil formation.

KEY RESEARCH ACCOMPLISHMENTS

- The Par-4 C-terminus is natively unfolded at physiological pH and temperature.
- Decrease in pH and temperature drastically affect the Par-4 C-terminal structure, inducing a switch from unfolded to a nearly fully coiled coil structure.
- Salt and peptide concentration also affect the conformational equilibrium. All data indicate a two-state equilibrium, affected by ionic contacts.
- Folded conformation is not monomeric, but represents a self-associated state.
- Chemical shifts of C-terminal peptide have been assigned, and relaxation and CSI data confirm little stable structure at high pH. These assignments will serve as a starting point for examining the relaxation and CSI data at lower pH.
- GST-pulldown assays indicate that the zinc-coordinating region of the atypical PKCs bind preferentially to the folded form of the Par-4 C-terminus. This is consistent with the subcellular localization of aPKC isoforms to the endosomal compartments.

REPORTABLE OUTCOMES

A manuscript has been accepted in Biotechniques (*20*), regarding development of the expression system used to produce the Par-4 peptides. This expression system combines the strengths of MBP fusion for solubility, His-tag for purification and a protease from human rhinovirus for efficient and specific fusion cleavage.

A second manuscript will be submitted shortly, regarding the CD spectroscopy and thermodynamic analysis discussed in the body. NMR studies will be published at a later date.

CONCLUSION

The Par-4 LZ region is required not only for homodimerization, but also for interaction with proposed effector proteins (see Introduction). It is through these interactions that Par-4 is thought to sensitize cells to apoptotic stimuli. But how does this natively unfolded region interact with effector proteins? First, the concentration dependence of the Par-4 LZ conformation may play a role. Overexpression of Par-4 enhances the potency of apoptotic stimuli in cells where Par-4 is constituitively expressed at lower levels (*2*). Higher concentrations in the cell could lead to a higher proportion of dimers. Dimerization and zipper formation could also be stabilized by interactions with or between other regions of the full length Par-4 protein. But it remains plausible that a considerable fraction of cellular Par-4 does not posses a stably folded C-terminus. However, a fully folded LZ may not be a requirement for interaction with effector proteins, which may be attracted to the unstructured acidic tail. The Par-4 LZ may be induced to fold only after complexation, or as part of the binding event. Examples of induced fold have been observed in many types of proteins, including those involved in transcriptional activation (*66-68*), RNA-binding (*69-71*), and cell cycle progression (*72, 73*). Pertinently, studies of conformationally unstable acidic LZ peptides have indicated an ability to form stable heterodimeric zippers with

basic LZ peptides at physiological pH, when the charge complimentarity of the synthetic peptides was carefully designed (*23*). Complimentary heterodimerization has also been seen with naturally occurring LZ sequences, such as Max/Myc (*58, 74*) and Jun/Fos (*75*). In fact, since attractive charge-charge interactions do not appear to be as important as the absence of repulsive charge-charge interactions, a LZ peptide with simply an absence of acidic residues in the *e* position may be capable of inducing heterodimerization with the PAR-4 C-terminus.

To date, interactions have not been detected between the Par-4 LZ and LZ regions of other proteins. The proposed cellular targets for the Par-4 LZ include the zinc-binding domains of the aPKCs and WT1, and an arginine-rich region of Dlk/ZIP kinase. The two names of the latter kinase signify homology with DAP kinase (Dap-Like-Kinase) (*76*) and the predicted presence of a C-terminal leucine zipper (ZIP) (*77*). Interestingly, the proposed LZ region of Dlk mediates interaction with LZ-containing transcription factors such as ATF-4 (*77*), but does not appear to be responsible for interaction with Par-4 (*13*). However, the Par-4 interacting region of Dlk kinase also possesses coiled coil propensity (~75% probability, as predicted by the program Multicoil (*78*)). This region may play the role of a basic LZ and heterodimerize with the PAR-4 LZ, or may interact in another manner due at least in part to charge complimentarity.

The pH-dependent behavior of the Par-4 LZ is consistent with the proposed interaction with the aPKCs. As opposed to other PKC isoforms, strong evidence has been presented for subcellular localization of the atypical PKCs to the lysosome-targetted endosomes (*79*). The acidic environment of these endosomes (pH ~ 5.0) is ideal for self-association of the Par-4 LZ. Although we were unable to gather CD data at low pH due to solubility constraints, conservative extrapolation of the inset plot in Figure 6 using a sigmoidal function predicts a T_m of 42 ± 4 °C at pH 5.0. Since folding as a function of temperature becomes increasingly cooperative at low pH (compare pH 6.25 and pH 5.5 curves in Figure 6) a T_m of 42 °C together with the projected shape of a pH 5.0 melting curve predicts a predominantly folded state at 37 °C. Thus in the endosomal compartment, Par-4 should be strongly self-associated, and would present a near fully folded coiled coil for interaction with the zinc-binding regulatory domain of the aPKCs. The GST pulldowns of Figure 11, showing that the zinc-coordinating domain of an aPKC interacts with the Par-4 C-terminus more strongly at low pH, is also consistent with this hypothesis. Precedent exists for induced folding in the endosomal environment: pH-dependent coiled coil formation of the influenza hemagglutinin protein in an endosomal environment has been linked to membrane fusion events critical for viral infection (*80-83*).

REFERENCES

1. Sells, S. F., Wood, D. P., Jr., Joshi-Barve, S. S., Muthukumar, S., Jacob, R. J., Crist, S. A., Humphreys, S., and Rangnekar, V. M. (1994) *Cell Growth & Differentiation 5*, 457-66.
2. Boghaert, E. R., Sells, S. F., Walid, A. J., Malone, P., Williams, N. M., Weinstein, M. H., Strange, R., and Rangnekar, V. M. (1997) *Cell Growth & Differentiation 8*, 881-90.
3. Guo, Q., Fu, W., Xie, J., Luo, H., Sells, S. F., Geddes, J. W., Bondada, V., Rangnekar, V. M., and Mattson, M. P. (1998) *Nature Medicine 4*, 957-62.
4. Duan, W., Guo, Z., and Mattson, M. P. (2000) *Experimental Neurology 165*, 1-11.
5. Mattson, M. P., Duan, W., Chan, S. L., and Camandola, S. (1999) *Journal of Molecular Neuroscience 13*, 17-30.
6. Kruman, II, Nath, A., Maragos, W. F., Chan, S. L., Jones, M., Rangnekar, V. M., Jakel, R. J., and Mattson, M. P. (1999) *American Journal of Pathology 155*, 39-46.
7. Pedersen, W. A., Luo, H., Kruman, I., Kasarskis, E., and Mattson, M. P. (1999) *Society of Neuroscience Abstracts 25*, 49.
8. Sells, S. F., Han, S. S., Muthukkumar, S., Maddiwar, N., Johnstone, R., Boghaert, E., Gillis, D., Liu, G., Nair, P., Monnig, S., Collini, P., Mattson, M. P., Sukhatme, V. P., Zimmer, S. G., Wood, D. P., Jr., McRoberts, J. W., Shi, Y., and Rangnekar, V. M. (1997) *Molecular & Cellular Biology 17*, 3823-32.
9. Zhang, Z., and DuBois, R. N. (2000) *Gastroenterology 118*, 1012-7.
10. Cook, J., Krishnan, S., Ananth, S., Sells, S. F., Shi, Y., Walther, M. M., Linehan, W. M., Sukhatme, V. P., Weinstein, M. H., and Rangnekar, V. M. (1999) *Oncogene 18*, 1205-8.
11. Diaz-Meco, M. T., Municio, M. M., Frutos, S., Sanchez, P., Lozano, J., Sanz, L., and Moscat, J. (1996) *Cell 86*, 777-86.
12. Johnstone, R. W., See, R. H., Sells, S. F., Wang, J., Muthukkumar, S., Englert, C., Haber, D. A., Licht, J. D., Sugrue, S. P., Roberts, T., Rangnekar, V. M., and Shi, Y. (1996) *Molecular & Cellular Biology 16*, 6945-56.
13. Page, G., Kogel, D., Rangnekar, V., and Scheidtmann, K. H. (1999) *Oncogene 18*, 7265-73.
14. Diaz-Meco, M. T., Lallena, M. J., Monjas, A., Frutos, S., and Moscat, J. (1999) *Journal of Biological Chemistry 274*, 19606-12.
15. Qiu, G., Ahmed, M., Sells, S. F., Mohiuddin, M., Weinstein, M. H., and Rangnekar, V. M. (1999) *Oncogene 18*, 623-31.
16. Camandola, S., and Mattson, M. P. (2000) *Journal of Neuroscience Research 61*, 134-9.
17. Nalca, A., Qiu, S. G., El-Guendy, N., Krishnan, S., and Rangnekar, V. M. (1999) *Journal of Biological Chemistry 274*, 29976-83.
18. Qiu, S. G., Krishnan, S., el-Guendy, N., and Rangnekar, V. M. (1999) *Oncogene 18*, 7115-23.
19. Barradas, M., Monjas, A., Diaz-Meco, M. T., Serrano, M., and Moscat, J. (1999) *EMBO Journal 18*, 6362-9.
20. Alexandrov, A., Dutta, K., and Pascal, S. M. (In press) *Biotechniques*.
21. Chen, Y. J., Yang, K., and Chan, K. (1974) *Biochemistry 13*, 3350-3359.
22. Seerama, N., and Woody, R. (1993) *Analytical Biochemistry 209*, 32-44.
23. Jelesarov, I., and Bosshard, H. R. (1996) *Journal of Molecular Biology 263*, 344-58.
24. Durr, E., Jelesarov, I., and Bosshard, H. R. (1999) *Biochemistry 38*, 870-80.
25. Marti, D. N., Jelesarov, I., and Bosshard, H. R. (2000) *Biochemistry 39*, 12804-18.

26. Delaglio, F., Grzesiek, S., Vuister, G. W., Zhu, G., Pfeifer, J., and Bax, A. (1995) *J. Biomol. NMR 6*, 277-293.
27. Johnson, B. A., and Blevins, R. A. (1994) *J. Biomol. NMR 4*, 603-614.
28. Jelesarov, I., Durr, E., Thomas, R. M., and Bosshard, H. R. (1998) *Biochemistry 37*, 7539-50.
29. Kohn, W. D., Monera, O. D., Kay, C. M., and Hodges, R. S. (1995) *Journal of Biological Chemistry 270*, 25495-506.
30. Krylov, D., Mikhailenko, I., and Vinson, C. (1994) *EMBO Journal 13*, 2849-61.
31. Marky, L. A., and Breslauer, K. J. (1987) *Biopolymers 26*, 1601-20.
32. Wishart, D. S., and Sykes, B. D. (1994) *J. Biomol. NMR 4*, 171-180.
33. Wishart, D. S., Sykes, B. D., and Richards, F. M. (1992) *Biochemistry 31*, 1647-1651.
34. Lupas, A. (1996) *Trends in Biochemical Sciences 21*, 375-82.
35. Lupas, A. (1997) *Current Opinion in Structural Biology 7*, 388-93.
36. Hicks, M. R., Holberton, D. V., Kowalczyk, C., and Woolfson, D. N. (1997) *Folding & Design 2*, 149-58.
37. Lumb, K. J., and Kim, P. S. (1995) *Biochemistry 34*, 8642-8.
38. Zeng, X., Herndon, A. M., and Hu, J. C. (1997) *Proceedings of the National Academy of Sciences of the United States of America 94*, 3673-8.
39. Harbury, P. B., Zhang, T., Kim, P. S., and Alber, T. (1993) *Science 262*, 1401-1407.
40. Gonzalez, L., Jr., Brown, R. A., Richardson, D., and Alber, T. (1996) *Nature Structural Biology 3*, 1002-9.
41. Gonzalez, L., Jr., Plecs, J. J., and Alber, T. (1996) *Nature Structural Biology 3*, 510-5.
42. Gonzalez, L., Jr., Woolfson, D. N., and Alber, T. (1996) *Nature Structural Biology 3*, 1011-8.
43. Potekhin, S. A., Medvedkin, V. N., Kashparov, I. A., and Venyaminov, S. (1994) *Protein Engineering 7*, 1097-101.
44. Spek, E. J., Bui, A. H., Lu, M., and Kallenbach, N. R. (1998) *Protein Science 7*, 2431-7.
45. O'Neil, K. T., and DeGrado, W. F. (1990) *Science 250*, 646-51.
46. Dahiyat, B. I., Gordon, D. B., and Mayo, S. L. (1997) *Protein Science 6*, 1333-7.
47. Krylov, D., Barchi, J., and Vinson, C. (1998) *Journal of Molecular Biology 279*, 959-72.
48. Zhou, N. E., Kay, C. M., and Hodges, R. S. (1994) *Journal of Molecular Biology 237*, 500-12.
49. Kohn, W. D., Kay, C. M., and Hodges, R. S. (1997) *Journal of Molecular Biology 267*, 1039-52.
50. Lavigne, P., Sonnichsen, F. D., Kay, C. M., and Hodges, R. S. (1996) *Science 271*, 1136-8.
51. Saudek, V., Pasley, H. S., Gibson, T., Gausepohl, H., Frank, R., and Pastore, A. (1991) *Biochemistry 30*, 1310-7.
52. Dyson, H. J., Rance, M., Houghten, R. A., Wright, P. E., and Lerner, R. A. (1988) *Journal of Molecular Biology 201*, 201-17.
53. Wendt, H., Leder, L., Harma, H., Jelesarov, I., Baici, A., and Bosshard, H. R. (1997) *Biochemistry 36*, 204-13.
54. Sosnick, T. R., Jackson, S., Wilk, R. R., Englander, S. W., and DeGrado, W. F. (1996) *Proteins 24*, 427-32.
55. Zitzewitz, J. A., Bilsel, O., Luo, J., Jones, B. E., and Matthews, C. R. (1995) *Biochemistry 34*, 12812-9.

56. Wendt, H., Berger, C., Baici, A., Thomas, R. M., and Bosshard, H. R. (1995) *Biochemistry 34*, 4097-107.
57. Ozeki, S., Kato, T., Holtzer, M. E., and Holtzer, A. (1991) *Biopolymers 31*, 957-66.
58. Lavigne, P., Kondejewski, L. H., Houston, M. E., Jr., Sonnichsen, F. D., Lix, B., Sykes, B. D., Hodges, R. S., and Kay, C. M. (1995) *Journal of Molecular Biology 254*, 505-20.
59. Muhle-Goll, C., Gibson, T., Schuck, P., Schubert, D., Nalis, D., Nilges, M., and Pastore, A. (1994) *Biochemistry 33*, 11296-306.
60. Yang, A. S., Gunner, M. R., Sampogna, R., Sharp, K., and Honig, B. (1993) *Proteins 15*, 252-65.
61. Anderson, D. E., Becktel, W. J., and Dahlquist, F. W. (1990) *Biochemistry 29*, 2403-8.
62. Lumb, K. J., and Kim, P. S. (1995) *Science 268*, 436-439.
63. Goto, Y., Calciano, L. J., and Fink, A. L. (1990) *Proc. Natl. Acad. Sci. USA 87*, 573-577.
64. Hendsch, Z. S., and Tidor, B. (1999) *Protein Science 8*, 1381-92.
65. Leberman, R., and Soper, A. K. (1995) *Nature 378*, 364-366.
66. Radhakrishnan, I., Perez-Alvarado, G. C., Parker, D., Dyson, H. J., Montminy, M. R., and Wright, P. E. (1997) *Cell 91*, 741-52.
67. Radhakrishnan, I., Perez-Alvarado, G. C., Dyson, H. J., and Wright, P. E. (1998) *FEBS Letters 430*, 317-22.
68. Kussie, P. H., Gorina, S., Marechal, V., Elenbaas, B., Moreau, J., Levine, A. J., and Pavletich, N. P. (1996) *Science 274*, 948-53.
69. Battiste, J. L., Mao, H. Y., Rao, N. S., Tan, R. Y., Muhandiram, D. R., Kay, L. E., Frankel, A. D., and Williamson, J. R. (1996) *Science 273*, 1547-1551.
70. Tan, R., and Frankel, A. D. (1994) *Biochemistry 33*, 14579-85.
71. Puglisi, J. D., Chen, L., Blanchard, S., and Frankel, A. D. (1995) *Science 270*, 1200-3.
72. Kriwacki, R. W., Hengst, L., Tennant, L., Reed, S. I., and Wright, P. E. (1996) *Proceedings of the National Academy of Sciences of the United States of America 93*, 11504-9.
73. Pavletich, N. P. (1999) *Journal of Molecular Biology 287*, 821-8.
74. Lavigne, P., Crump, M. P., Gagne, S. M., Hodges, R. S., Kay, C. M., and Sykes, B. D. (1998) *Journal of Molecular Biology 281*, 165-81.
75. O'Shea, E. K., Rutkowski, R., Stafford, W. F., 3rd, and Kim, P. S. (1989) *Science 245*, 646-8.
76. Kogel, D., Plottner, O., Landsberg, G., Christian, S., and Scheidtmann, K. H. (1998) *Oncogene 17*, 2645-54.
77. Kawai, T., Matsumoto, M., Takeda, K., Sanjo, H., and Akira, S. (1998) *Molecular & Cellular Biology 18*, 1642-51.
78. Wolf, E., Kim, P. S., and Berger, B. (1997) *Protein Science 6*, 1179-89.
79. Sanchez, P., De Carcer, G., Sandoval, I. V., Moscat, J., and Diaz-Meco, M. T. (1998) *Molecular & Cellular Biology 18*, 3069-80.
80. Bullough, P. A., Hughson, F. M., Skehel, J. J., and Wiley, D. C. (1994) *Nature 371*, 37-43.
81. Carr, C. M., and Kim, P. S. (1993) *Cell 73*, 823-32.
82. Chen, J., Skehel, J. J., and Wiley, D. C. (1999) *Proceedings of the National Academy of Sciences of the United States of America 96*, 8967-72.
83. Weissenhorn, W., Dessen, A., Harrison, S. C., Skehel, J. J., and Wiley, D. C. (1997) *Nature 387*, 426-30.

BIBLIOGRAPHY

Alexandrov, A., Dutta, K., Pascal, S. M. "MBP-fusion with a viral protease cleavage site: one-step cleavage/purification of insoluble proteins", *Biotechniques*, in press.

Dutta, K., Alexandrov, A., Huang, H., Pascal S. M. "A natively unstructured apoptotic domain forms a pH-induced leucine zipper", in preparation.

PERSONNEL RECEIVING PAY

Steven M. Pascal, Ph.D.
Kaushik Dutta, Ph.D.
Huang He, Ph.D.
Andrei Alexandrov, M.S.

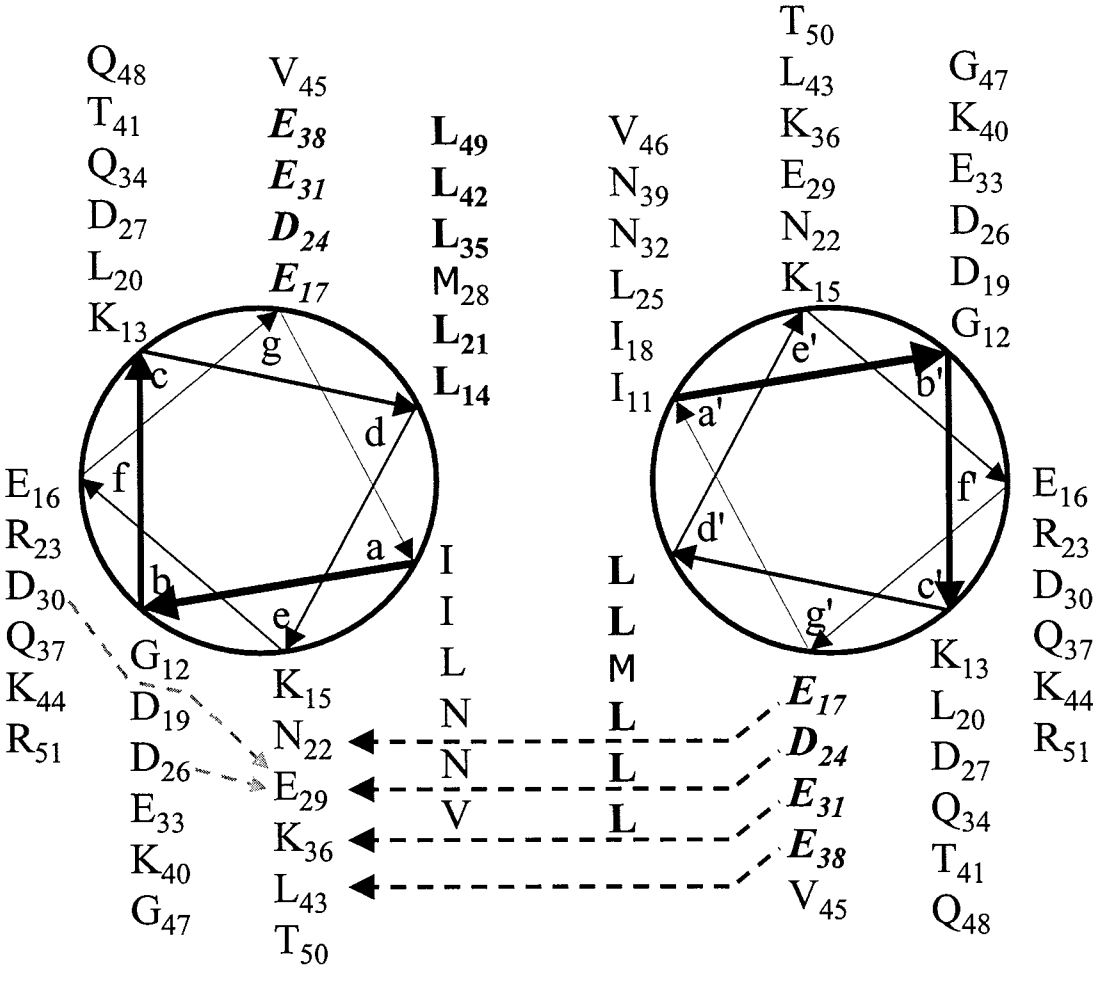

Figure 1. The Par-4 LZ peptide. (a) Primary sequence. Residues 5-51 represent Par-4 residues 286-332. Positions in heptad repeat are dentoted below by *abcdefg*. (b) Helical wheel representation. The Leucine repeat at the *d* position is shown in bold, and the acidic repeat at the *g* position is in bold italics. The potential *g'* → *e* interactions involving the acidic *g'* repeat are shown as dark dashed arrows. Lighter dashed arrows indicate possible intramolecular charge-charge repulsions involving E29.

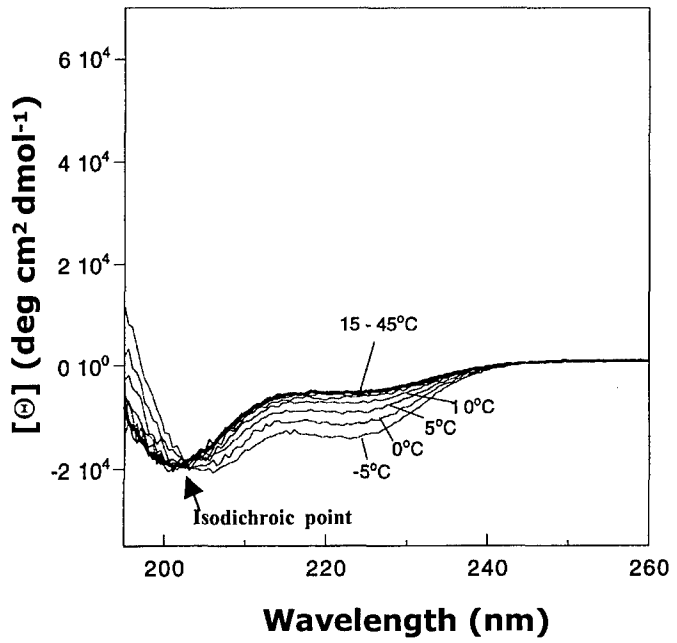

Figure 2. Far UV CD spectra of Par-4 LZ peptide as a function of temperature in 12 mM NaP, 20 mM NaCl, pH 6.5. The dark trace was recorded at 25 °C. Peptide concentration was 22 μM.

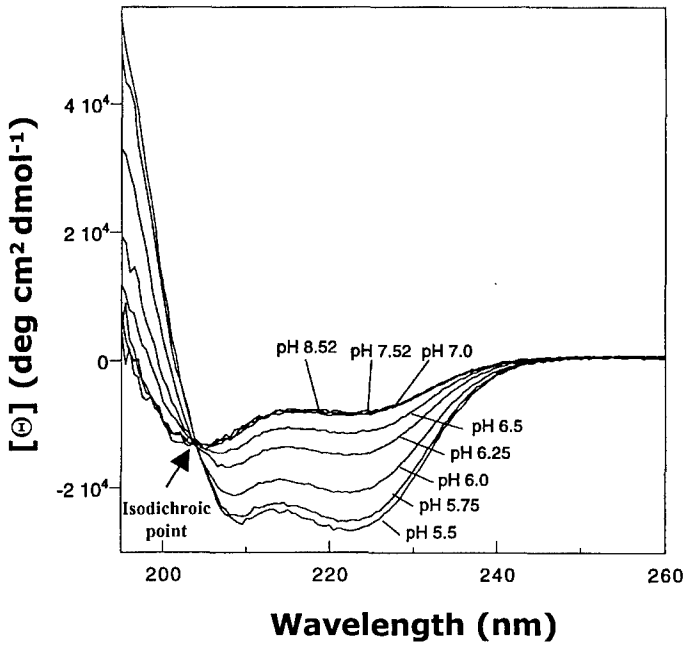

Figure 3. Far UV CD spectra of Par-4 LZ as a function of pH in 12 mM NaP, 140 mM NaCl, 5 °C. Peptide concentration was 22 μM.

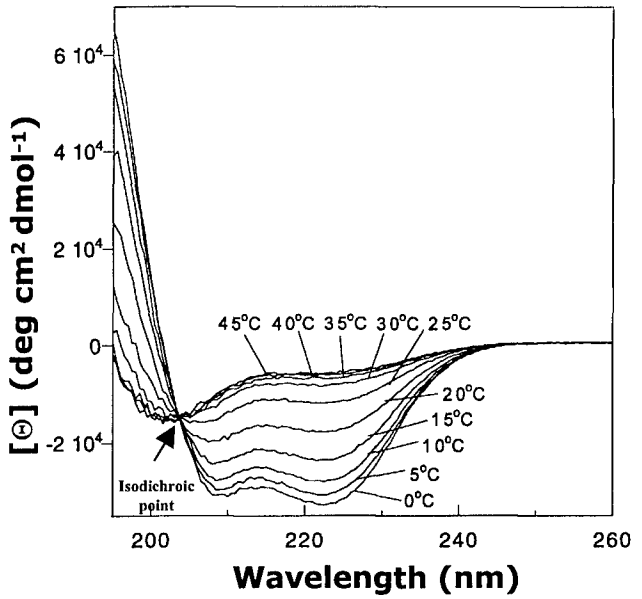

Figure 4. Far UV CD spectra of Par-4 LZ as a function of temperature in 12 mM NaP, 20 mM NaCl, pH 5.75. Peptide concentration was 27 μM.

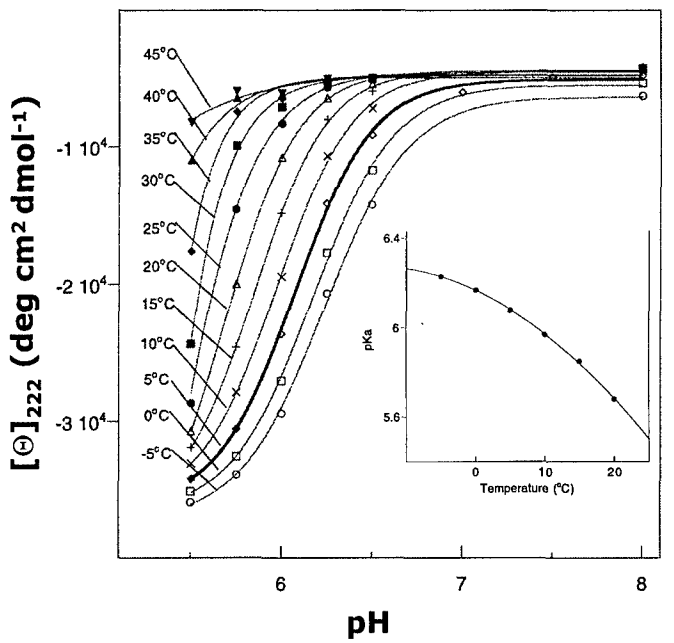

Figure 5. pH dependence of the molar ellipticity $[\theta]_{222}$ of Par-4 LZ as a function of temperature. These curves were fit to equation 1 to extract the conformational pKa (inset) and Hill coefficient as functions of temperature (see Table 1). Sample was 18 μM peptide in 12 mM NaP, 20 mM NaCl.

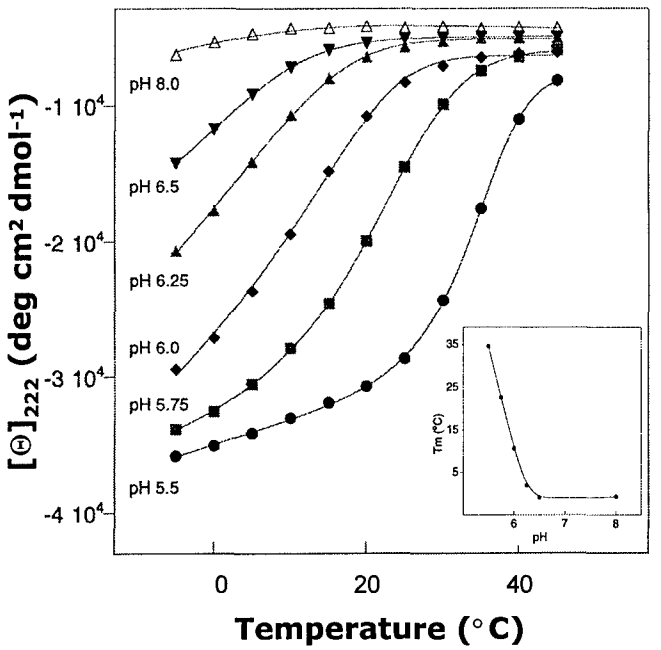

Figure 6. Temperature dependence of the molar ellipticity $[\theta]_{222}$ of Par-4 LZ as a function of pH. These curves were fit to the modified equation 5 to extract the T_m (inset) and ΔH_m as functions of pH (see Table 2). Sample was 18 μM peptide in 12 mM NaP, 20 mM NaCl.

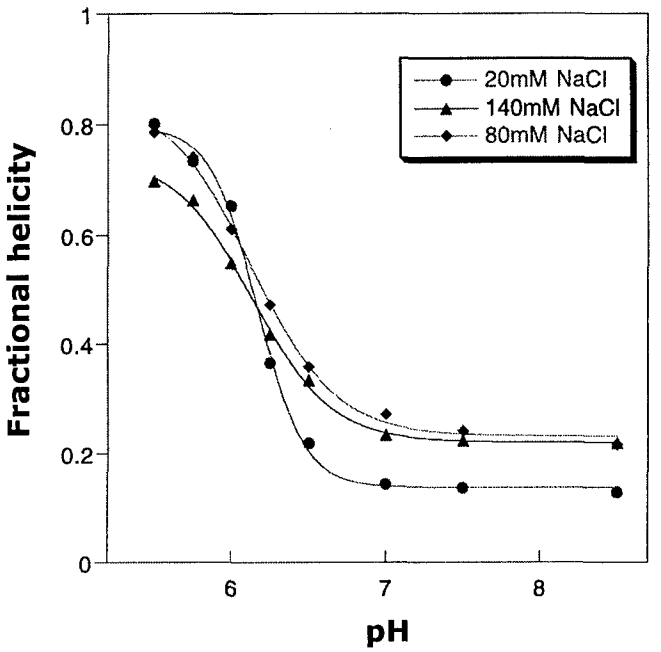

Figure 7. The fractional helicity of Par-4 LZ vs. pH at three different salt concentrations. Sample was 27 μM peptide in 12mM NaP, 5°C.

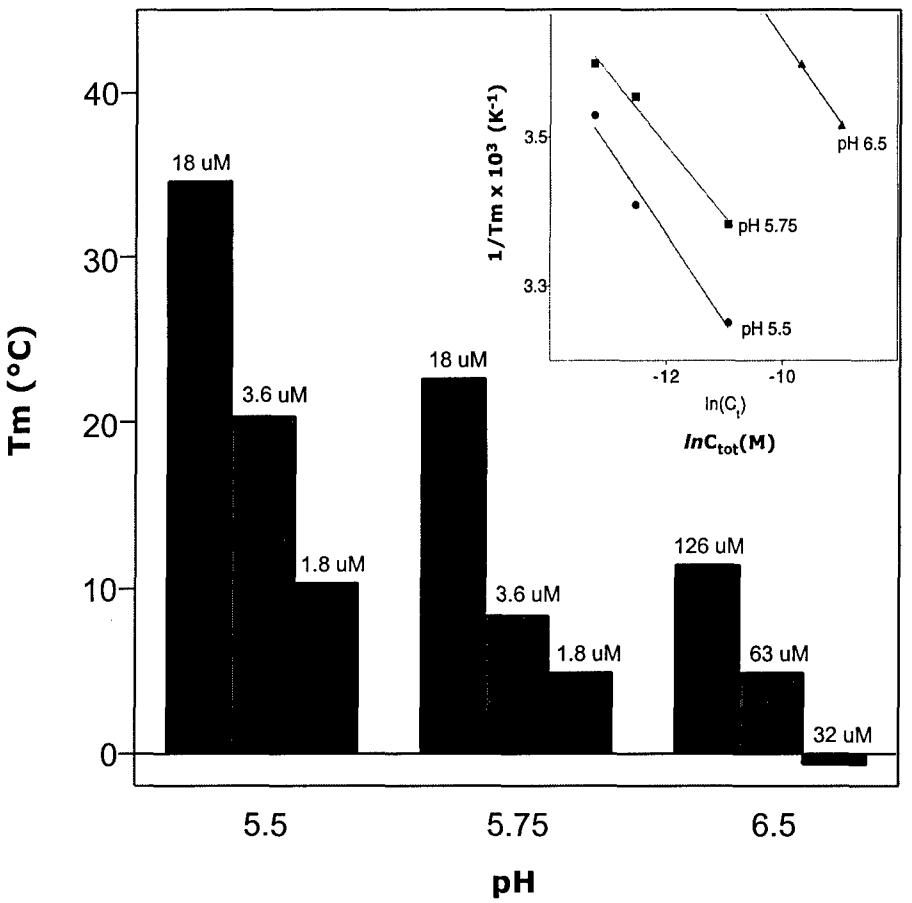

Figure 8. Variation of T_m vs. total PAR-4 LZ concentration at three different pH values. $1/T_m$ vs. natural log of concentration is plotted in the inset. Sample was in 12 mM NaP, 20mM NaCl.

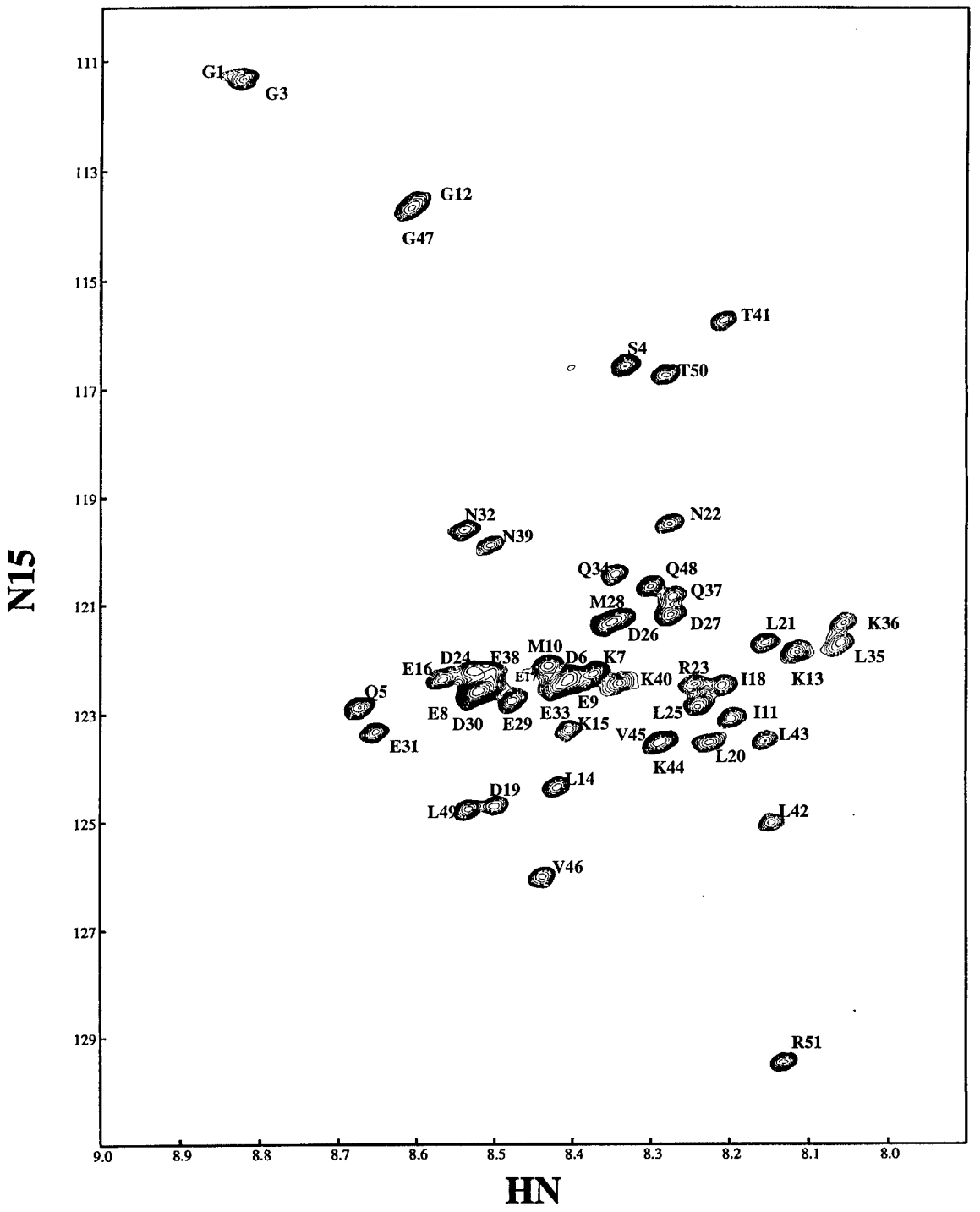

Figure 9. $^{1}H,^{15}N$-HSQC spectrum of Par-4 LZ with residue specific assignments.

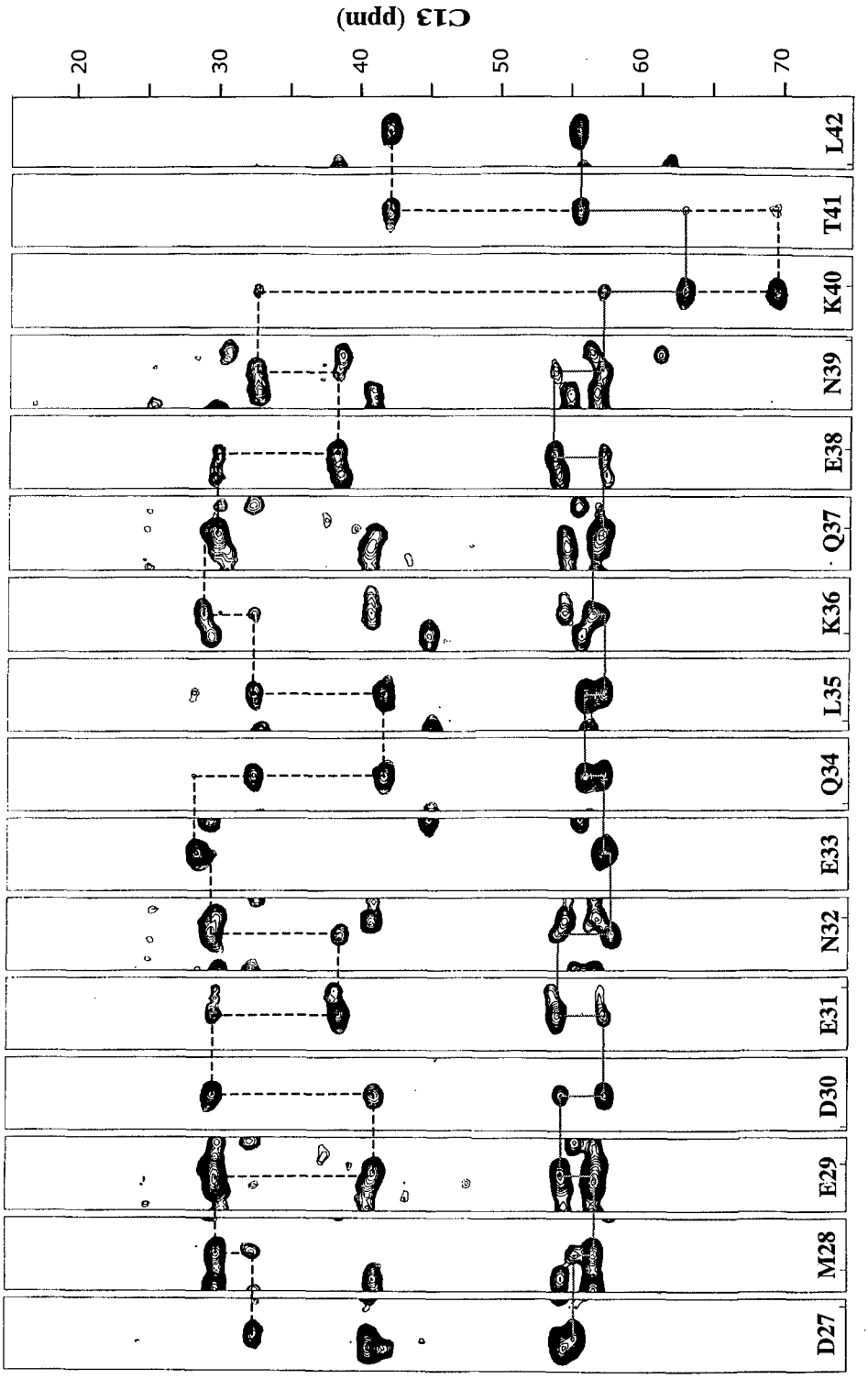

Figure 10. HNCACB strip plots illustrating backbone chemical shift assignment of Par-4 LZ.

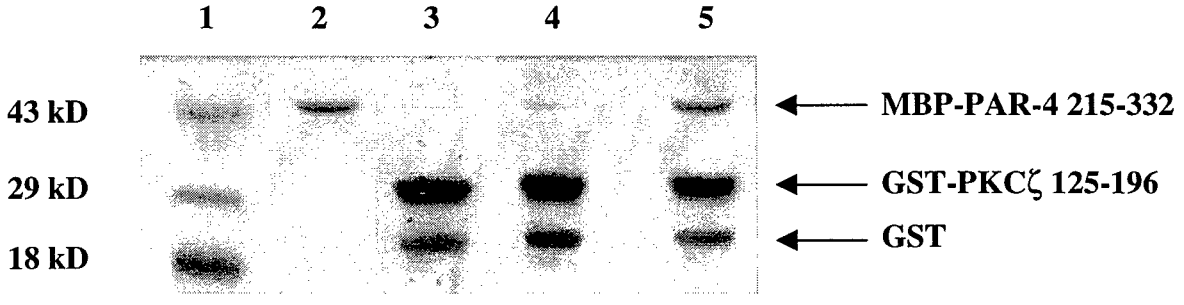

Figure 11. In order to detect interactions between Par-4 and PKC domains, purified MBP -Par-4 (residues 215-332) was incubated with GST-PKC-zeta (residues 125-196) which was immobilized on gluthatione beads. After co-incubation for 2 hrs. in 12mM NaP_i, 140mM NaCl, 5mM βME, 5mM $ZnCl_2$ at 4°C, the beads were throughly washed and then boiled in SDS buffer for 10 minutes. The GST-PKC-zeta along with any associated Par-4 fusion were then fractionated by SDS PAGE. ***(1)*** Molecular Weight Markers; ***(2)*** Input MBP-PAR-4 (215-332); ***(3)*** Immobilized GST-PKCζ 125–196 before addition of MBP-Par-4 (215-331); ***(4)*** Co-incubation of PAR-4 and PKC fusions at pH 7.5; ***(5)*** Co-incubation of PAR-4 and PKC fusions at pH 3.5.

Table 1. pKa and Hill coefficients extracted by fitting the curves from Figure 5 to equation 1.

Temp. (°C)	pKa	Hill coefficient
-5	6.23 ± 0.02	1.88 ± 0.17
0	6.17 ± 0.02	1.95 ± 0.17
5	6.08 ± 0.02	2.04 ± 0.15
10	5.97 ± 0.02	2.10 ± 0.15
15	5.85 ± 0.02	2.22 ± 0.13
20	5.69 ± 0.03	2.15 ± 0.17
25	5.41 ± 0.14	2.02 ± 0.41
30	5.47 ± 0.50	2.22 ± 1.40
35	5.51 ± 0.84	2.55 ± 3.30

Table 2. Thermodynamic parameters extracted from fitting thermal denaturing curves, including those presented in Figure 6, to the modified equation 5 described in the text. Fitting was performed at three different salt concentraions, six different pH values and several Par4 –LZ concentrations.

Salt (mM)	pH	C_{tot} (μM)	T_m (K)	ΔH_m (kJ/mol)
20	5.5	18	307.6 ± 0.1	322.8 ± 10.1
		3.6	293.4 ± 1.6	127.6 ± 11.4
		1.8	283.3 ± 3.8	108.1 ± 14.6
	5.75	18	295.7 ± 0.4	191.9 ± 6.8
		3.6	281.3 ± 1.8	128.6 ± 8.5
		1.8	277.9 ± 9.9	105.8 ± 26.0
	6.0	18	283.6 ± 0.6	142.0 ± 3.6
	6.25	18	275.0 ±0.5	125.0 ± 1.6
	6.5	126	284.4 ± 0.6	165.8 ± 6.2
		63	277.9 ± 0.9	134.1 ± 3.6
		32	272.5 ± 0.7	120.8 ± 1.4
		18	272.1 ± 1.5	129.4 ± 3.1
	8	18	272.3 ± 6.8	108.5 ± 44.5
80	5.5	22	304.7 ± 0.6	138.9 ± 12.3
	5.75	22	294.1 ± 0.2	209.1 ± 5.0
		4.4	286.6 ± 1.2	164.5 ± 9.1
	6.0	120	298.6 ± 0.2	260.7 ± 9.0
		22	285.3 ± 0.4	167.1 ± 4.1
		12	281.3 ± 1.0	147.4 ± 6.3
	6.25	22	281.2 ± 0.6	163.7 ± 4.0
	6.5	22	277.7 ± 0.4	150.9 ± 1.8
	8	22	276.8 ± 1.7	113.1 ± 17.7
140	5.5	22	305.7 ± 0.2	245.3 ± 10.9
	5.75	22	297.3 ± 0.2	226.5 ± 5.6
	6.0	22	289.5 ± 0.6	194.6 ± 10.0
	6.25	22	281.2 ± 2.0	153.7 ± 10.2
	6.5	22	279.9 ± 0.8	150.0 ± 4.0
	8	22	278.9 ± 2.3	139.5 ± 8.8

Table 3. Chemical shift assignment of Par4 LZ

	HN	N	CO	Ca	Cb	Cg	Cd	Ce	Ha	Hb	Hg	Hd	He
G1	8.85	111.32							4.01				
P2			177.63	63.516	32.31	27.19	49.69		4.5	2.34/2.02			
G3	8.82	111.34	174.47	45.245					4.03				
S4	8.33	116.61	174.93	58.613	63.76				4.46	3.93/3.89			
Q5	8.67	122.89	175.86	55.993	29.34	33.93			4.35	2.11/1.99	2.37		
D6	8.4	122.38	176.45	54.744	41.13				4.57	2.74/2.63			
K7	8.37	122.28	176.83	56.85	33.01	24.70	42.22		4.27	1.86/1.79	1.44	1.69	
E8	8.53	122.65	176.89	56.953	30.31	36.45			4.26	1.99	2.38/2.27		
E9	8.4	122.5	176.78	56.837	30.34	36.33			4.24		2.23		
M10	8.43	122.13	176.55	55.714	32.65	29.01	33.95		4.49	2.11/2.04			
I11	8.2	123.11	177.78	61.883	38.5	17.42/27.51	72.64		4.14	1.88			
G12	8.6	113.56	174.24	45.452					3.94				
K13	8.11	121.9	176.91	56.39	33.31	24.81	29.33		4.33	1.89/1.78			
L14	8.42	124.38	177.72	55.431	42.3	27.16	24.96/23.41		4.32	1.67/1.60	1.61	.94/.88	
K15	8.4	123.31	176.78	57.035	32.97	24.80			?				
E16	8.57	122.38	176.59	56.642	30.41	36.28			4.25	2.06/1.98	2.3/2.26		
E17	8.47	122.32	176.96	56.877	30.29	36.31			4.28				
I18	8.21	122.5	176.32	61.77	38.93	17.58/27.6	72.78		4.14	1.89			
D19	8.5	124.73	176.55	54.658	41				4.26	2.74/2.64			
L20	8.22	123.55	174.93	55.858	42.21	27.03	25.14/23.43		4.27	1.68/1.61	1.62	.94/.88	
L21	8.15	121.72	176.55	55.649	42.07	27.04	23.48/24.94		4.3	1.68/1.59	1.62	.94/.87	
N22	8.28	119.52	175.26	53.347	38.8				4.7	2.87/2.75			
R23	8.24	122.48	176.16	56.383	30.97	26.94		43.4	?	?			
D24	8.53	122.23	176.55	54.727	40.98				4.58	2.74/2.64			
L25	8.24	122.89	177.6	55.494	42.23	27.06	25.19/23.28		4.33	1.67/1.60	1.66	.95/.88	
D26	8.36	121.36	176.19	54.745	41.13				4.59	2.73/2.63			
D27	8.27	121.21	176.42	54.494	41				4.59	2.75/2.64			
M28	8.34	121.26	176.62	55.638	32.83	32.13			4.47	2.12/2.03	2.63/2.54		
E29	8.48	122.77	176.96	56.873	30.27	36.32			4.24				
D30	8.51	122.58	176.9	54.552	41.38				4.58	2.74/2.65			
E31	8.65	123.34	176.98	57.579	29.99	36.17			4.21	2.07/2.01			
N32	8.54	119.63	176.33	54.145	38.88				4.66	2.86			
E33	8.42	122.52	177.68	58.039	29.77	36.03			4.15	2.32/2.08			
Q34	8.35	120.46	177.33	57.388	28.77	33.90			4.18	2.30/1.92			
L35	8.06	121.72	178.2	56.155	41.98	27.08	24.89/23.61		4.27	1.71/1.61			
K36	8.05	121.36	177.63	57.365	32.81	25.07	29.41	42.11	4.23				
Q37	8.28	120.87	176.83	56.42	29.21	33.71			4.26	2.14/2.05			
E38	8.5	122.21	176.82	57.349	30.16	36.24			4.21	2.3/2.15			
N39	8.51	119.91	175.88	53.68	38.57				4.69	2.87/2.81			
K40	8.34	122.46	177.34	57.126	32.88	25.01	29.25	42.22	4.22				
T41	8.21	115.74	174.7	62.938	69.52	21.75			4.25	4.22	1.22		
L42	8.15	125.04	177.29	55.398	42.24	27.05	23.6/24.94		4.34	1.67/1.61			
L43	8.16	123.53	177.26	55.218	42.25	26.99	23.59/24.91		4.38	1.64/1.62			
K44	8.29	123.58	176.45	56.279	33.07	24.91	29.14	41.08	4.32	1.79			
V45	8.29	123.49	176.4	62.331	32.91	21.03			4.12	2.04	0.94		
V46	8.44	126.03	176.84	62.869	32.77	21.02			4.1	2.07	0.98		
G47	8.61	113.67	173.93	45.211					3.96				
Q48	8.3	120.7	176.08	55.765	29.78	33.81			4.3	2.11/1.99			
L49	8.53	124.78	177.62	55.287	42.45	27.08	24.95/23.51		4.45	1.69/1.63		.94/.89	
T50	8.28	116.76	173.64	61.841	70.08	21.66			4.37	4.24	1.22		
R51	8.13	129.48		57.483	31.47								

DEPARTMENT OF THE ARMY
US ARMY MEDICAL RESEARCH AND MATERIEL COMMAND
504 SCOTT STREET
FORT DETRICK, MD 21702-5012

REPLY TO
ATTENTION OF

MCMR-RMI-S (70-1y) 15 May 03

MEMORANDUM FOR Administrator, Defense Technical Information Center (DTIC-OCA), 8725 John J. Kingman Road, Fort Belvoir, VA 22060-6218

SUBJECT: Request Change in Distribution Statement

1. The U.S. Army Medical Research and Materiel Command has reexamined the need for the limitation assigned to technical reports written for this Command. Request the limited distribution statement for the enclosed accession numbers be changed to "Approved for public release; distribution unlimited." These reports should be released to the National Technical Information Service.

2. Point of contact for this request is Ms. Kristin Morrow at DSN 343-7327 or by e-mail at Kristin.Morrow@det.amedd.army.mil.

FOR THE COMMANDER:

Encl

PHYLIS M. RINEHART
Deputy Chief of Staff for
Information Management

ADB266022
ADB260153
ADB272842
ADB283918
ADB282576
ADB282300
ADB285053
ADB262444
ADB282296
ADB258969
ADB269117
ADB283887
ADB263560
ADB262487
ADB277417
ADB285857
ADB270847
ADB283780
ADB262079
ADB279651
ADB253401
ADB264625
ADB279639
ADB263763
ADB283958
ADB262379
ADB283894
ADB283063
ADB261795
ADB263454
ADB281633
ADB283877
ADB284034
ADB283924
ADB284320
ADB284135
ADB259954
ADB258194
ADB266157
ADB279641
ADB244802
ADB257340
ADB244688
ADB283789
ADB258856
ADB270749
ADB258933
ADB265793
ADB281613
ADB284934
ADB263442
ADB284977
ADB263437
ADB265310
ADB281573
ADB250216
ADB258699
ADB274387
ADB285530